

PHOTO-INDUCED FORMATION OF SURFACE RELIEF IN AMORPHOUS As_2S_3 FILMS*

ELINA POTANINA*, JANIS TETERIS

Institute of solid State Physics, University of Latvia, LV 1063 Riga, Latvia

In this report we study the formation of surface relief in arsenic trisulphide films under laser light radiation. Recording was performed with only one laser beam with lateral modulated polarisation direction. The photo-induced changes on the surface were initiated by DPSS laser light (532 nm). The formation process was studied measuring the depth and profile of recorded surface relief. Results are presented graphically as reliefs' depth dependence on various recording parameters (polarisation configuration, exposure doze and recording geometry).

(Received October 3, 2013; Accepted November 11, 2013)

Keywords: Surface relief gratings, Photo-induced mass transport, Optical recording.

1. Introduction

Structure like surface relief grating (SRG) can be used as diffractive optical element and as Bragg reflector. The one beam method was used to study SRG formation in chalcogenide films. Well-known chalcogenide – amorphous arsenic trisulphide was used for this purpose. As_2S_3 is known as inorganic polymer, which is often used in holography due to large photo-induced changes of its chemical and optical properties [1.2.3]. It has been studied since 1950' and a lot of interesting optical phenomena [1.2.3.4.5.6] like photoexpansion, photodarkening, photo-induced dichroism and birefringence were discovered. However, there are things still to discuss - photo-induced mass transport. Studying SRG formation process mainly consists of finding appropriate conditions for efficient photo-induced mass transport. Surface relief can be obtained with holographic record as well as by illumination through optical slit [8.9], but this study is based on one beam record. Since there is no interference, set-up is stable to vibrations and there is no need in high coherence of recording light source. Experimental set-up consisting of polarisation direction modulator, half-wave plates and lenses is shown in Fig 1.

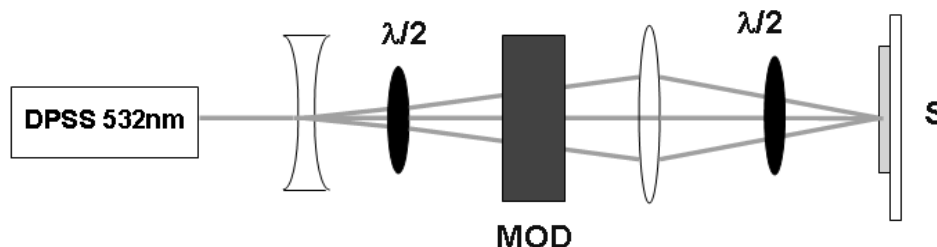


Fig. 1. Experimental set-up for recording surface relief grating with one beam method.

L - lens; $\lambda/2$ – half-wave plate; MOD – polarisation modulating element; S – sample.

Recording was performed with DPSS laser $\lambda = 532\text{nm}$.

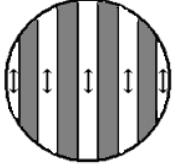
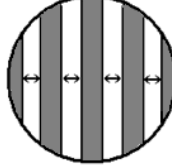
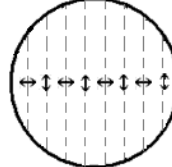
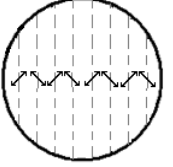
*Paper presented at 6th International Conference on Amorphous and Nanostructured Chalcogenides, Brasov, Romania, June 24-28, 2013

* Corresponding author: elina.potanina@gmail.com

2. Experimental

Surface relief gratings (SRG) are usually recorded using holographic method what is based on two beam interference [8.9]. Depending on recording beam polarisation direction it can provide an interference pattern with light intensity and polarisation distribution what is necessary for SRG formation. In this study we observe formation of surface relief using only one beam. Method is based on modulating light polarisation direction in one laser beam. In this case intensity pattern on samples' surface is quite similar to interference pattern. By using MOD and half-wave plate polarisation is modulated according to already known configurations. For example, the S-S configurations' analogue in holography is interference of two linearly S - polarised waves. Modulated polarisation directions in one laser beam and its analogous examples in holography are shown in Table 1.

Table 1. Simplified scheme of polarisation distribution

	S-S	P-P	S-P	45⁰; -45⁰
1				
2	Interference of two S-polarised waves	Interference of two P-polarised waves	Interference of R and L (or 45 ⁰ ; -45 ⁰) polarised waves	Interference of S and P-polarised waves

↑ - electric field vector oscillation direction

1 – Modulated polarisation direction in one laser beam.

2 – Similar distribution obtained with two beams (holographic analogy).

For direct SRG record amorphous arsenic trisulphide films were used as photoresists. Samples with different thickness (from 1µm to 10µm) were prepared by vacuum evaporation onto glass substrate.

Surface reliefs were recorded using modulated DPSS laser beam with 532 nm wavelength.

Intensity of laser beam was constant during the recording $\sim 4 \text{ W/cm}^2$. SRGs were recorded with a constant period – 50 µm. Depth and profile of recorded SRG was measured with profilometer. To change polarisation configuration the second half-wave plate is rotated, but S-S or P-P configuration is obtained by inserting polarising cube after the second half-wave plate.

3. Results and discussion

SRG recorded with different polarisation modulations was studied first. Recording with all four configurations gave positive results (Figure 2.), but SRG recorded with S-P modulation was the deepest.

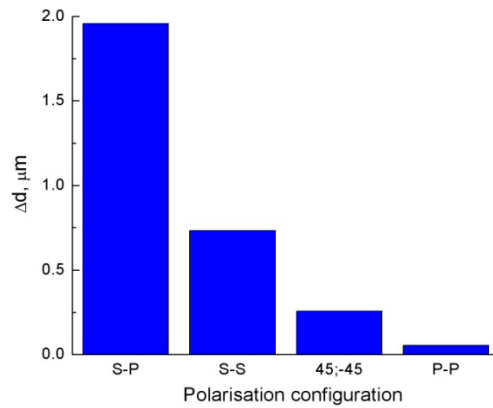


Fig. 2. Depth (Δd) of SRG recorded with according polarization modulation

Intensity distribution is the same for S-P and $45^0;-45^0$, but the results differ ~ 8 times. S-S and P-P configurations are similar, but still there is a big difference in results. It means that electric field vector oscillation direction is principal photo-induced mass transport mechanism. In SRG formation process polarisation modulation plays the key role. It provides electric field gradient [8] what induces mass transport. S-P configuration in one beam method is analogue of $45^0;-45^0$ polarisation state in holography.

The velocity of mass transport process is not constant and growth of SRG is not infinite process. SRG formation process, increasing exposure, is shown in Fig. 3. SRG formation process consists of two parts: fast growth ($t = [0...12]$ h) and saturation process, the part of slow growth ($t = [12...70]$ h). It supposes to reach the maximum, i.e., biggest possible SRG depth value. Thinner films are most likely to reach the maximum faster, because there is same amount of received energy, but less mass to transfer. Form of graphic, process tendency, is the same for all three films with different thickness. Recording SRG in $1 \mu\text{m}$ thick film is possible at smaller exposure or intensity. At $t \approx 10$ h and $I \approx 4 \text{ W/cm}^2$ SRG starts to disband. Damage of SRG can be caused by large amount of received energy, illuminated area heating or large period influence.

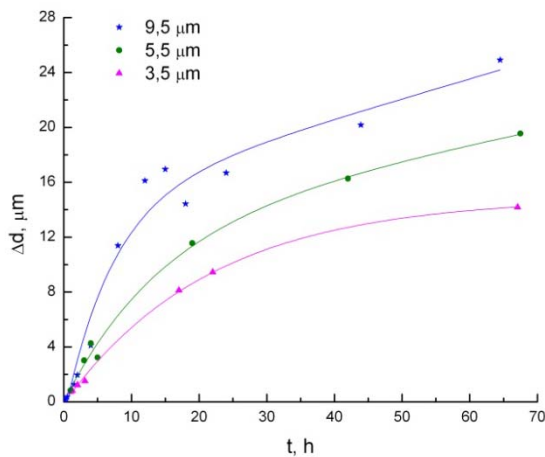


Fig. 3. SRG depth dependence on exposure. Δd – SRG depth in micrometers. Samples with thicknesses $3.5 \mu\text{m}$, $5.5 \mu\text{m}$ and $9.5 \mu\text{m}$ were used. Recording beam intensity $\sim 4 \text{ W/cm}^2$. Second order exponential decay function is used to fit experimental data.

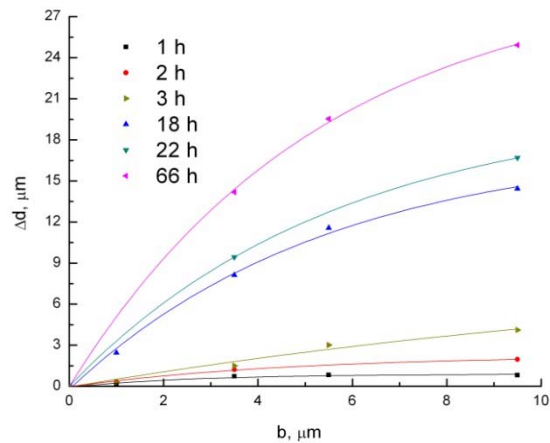


Fig. 4. SRG depth dependence on film thickness at different exposures; Δd – SRG depth in micrometers; b – film thickness in micrometers. Exponential fit is used.

Depth of recorded SRG depends on films thickness, too. SRG formation process versus film thickness is shown in Figure 4. Process seems to be exponentially growing. To evaluate the

effectiveness of each thickness, the ratio $\frac{\Delta d}{b}$ was calculated. Most efficient film thicknesses are from 3.5 μm to 5.5 μm , with value of ratio 0.21 (1 h exposure) – 4.05 (66 h exposure). For thicker films, as there is a lot of mass to transport, process is slower and they are efficient at long exposures. Deeper SRG can be recorded, but it takes more time.

SRG formation process depends on amount of received energy. Next step contains study of SRG depth recorded with constant dose ($It = \text{const}$). Increasing recording beam intensity and decreasing exposure so dose value stays constant shouldn't cause any changes in SRG depth. Practically, SRG depth value does not change within the range. It is limited by intensity values: [0.5 – 7.5] W/cm^2 (Figure 5.). Formation process consists of material softening first. There is some amount of energy what is necessary for chemical bond disruption process and it is limiting factor at low intensity range. Bond disruption is possible because of selected recording beam wavelength as photon energy value (~ 2.34 eV) is close to As_2S_3 band gap (2.4 eV). Studying low intensity range and decreasing intensity value the probability of bond disruption decreases (1).

$$I \sim A^2 \quad (1)$$

If bond disruption probability decreases, then material in the illuminated area is softening slower and velocity of SRG formation process decreases (Figure 5.a.).

Explanation of SRG depth increase at high intensity range needs more studies of SRG recorded with intensity greater than 11 W/cm^2 .

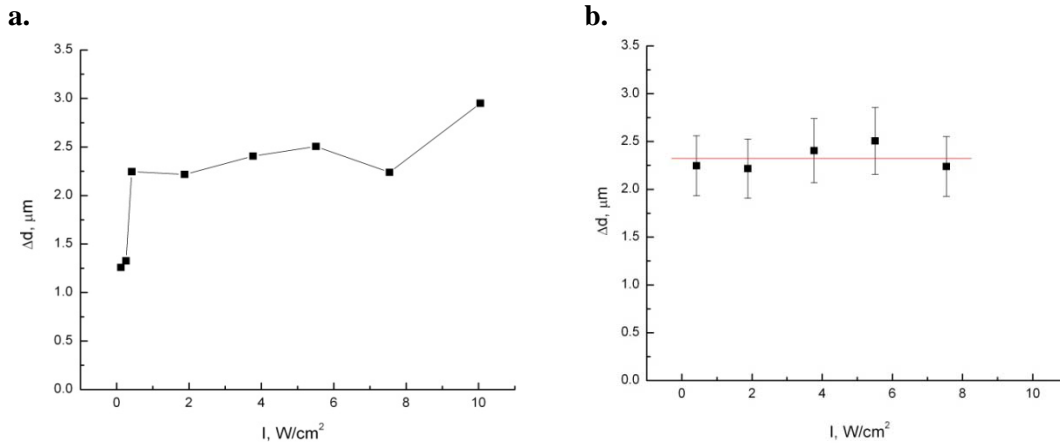


Fig. 5. a. SRG depth dependence on intensity ($It = \text{const}$)
b. linear part with $\Delta d = \text{const}$

SRG depth dependence on geometry of sample illumination has been studied, too. Recording from substrate and film side was compared (Figure 6). Recording SRG from substrate side provides different intensity distribution in the material and prevents heating and melting of structure peaks. Formation process is slower in the beginning at smaller exposure values, but after 8 hours (with intensity ~ 4 W/cm^2) higher SRG can be obtained. For faster and efficient results recording beam intensity can be increased.

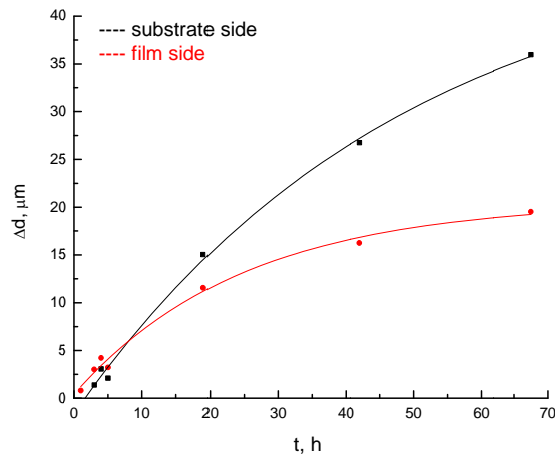


Fig. 6. Depth of SRG recorded from --- film and --- substrate side. Film thickness 5,5 μm

Changing geometry of sample illumination does not affect the form of recorded structure. Example of recorded SRGs and its profiles are shown in Fig. 7a, 7b.

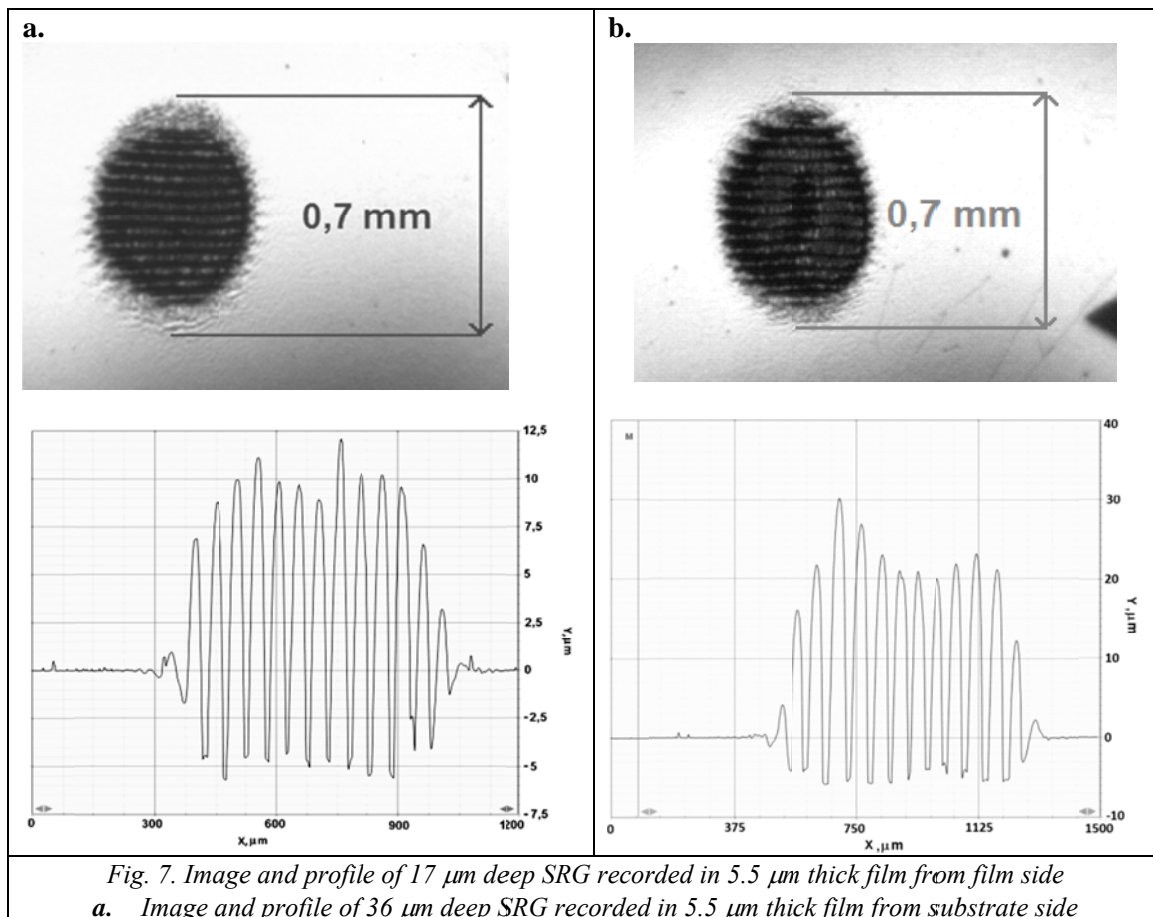


Fig. 7. Image and profile of 17 μm deep SRG recorded in 5.5 μm thick film from film side
 a. Image and profile of 36 μm deep SRG recorded in 5.5 μm thick film from substrate side

4. Conclusions

The one beam method is applicable for studying photo-induced mass transport in chalcogenide films. It is easier and cheaper way of recording SRG then holographic record. Efficient recording parameters have been found:

- S-P polarization configuration (holographic analogy 45^0 ; -45^0) is necessary.

- For recording large period (50 μm) SRG optimal film thickness is $\sim 4.5 \mu\text{m}$.
- Deeper structures can be obtained recording SRG from substrate side.

Acknowledgements

This work has been supported by ERAF project
r.2010/0204/2DP/2.1.1.2.0/10/APIAA/VIAA/010.

References

- [1] H. Hisakuni, K. Tanaka, , Appl. Phys. Lett. **65**(23), 2925 (1994).
- [2] A. Kolobov, K. Tanaka, , in Handbook of Advanced Electronic and Photonic Materials and Devices, Vol. **5**, H.S. Nalwa (Ed.), Academic Press, San Diego, p.47. (2001)
- [3] K. Tanaka, J. Non-Cryst. Solids **35&36**, 1073 (1980).
- [4] A. Roy, A.V. Kolobov, K. Tanaka J. Appl. Phys. **83**, 4951 (1998).
- [5] K. Tanaka, , in Handbook of Advanced Electronic and Photonic Materials and Devices, Vol. **5**, H.S. Nalwa (Ed.), Academic Press, San Diego, p.120 (2001).
- [6] K. Tanaka, N. Terakado, A. Saitoh J. Optoelectron. Adv. Mater. **10**(1), 124 (2008).
- [7] J. Hajito, I. Janossy Phil. Mag. B **47**(4), 347 (1983).
- [8] U. Gertners, J. Teteris, , J. Optoelectron. Adv. Mater. **13**(11-12), 1462 (2011)
- [9] U. Gertners, J. Teteris, , IOP Conf. Series: Mater. Science and Engineering, **38**, 012026 (2012).